

# Experimental Study of The Performance of a Solar Chimney Power Plant Model in Basrah City

Qais A. Rishak, Hussien S. Sultan, Ihsan N. Jawad

Department of Mechanical Engineering, College of Engineering, University of Basrah

\*Corresponding Author Email: [ihsanynandhim@gmail.com](mailto:ihsanynandhim@gmail.com), [qais.rashck@uobasrah.edu.iq](mailto:qais.rashck@uobasrah.edu.iq)  
[hussien.sultan@uobasrah.edu.iq](mailto:hussien.sultan@uobasrah.edu.iq)

## ABSTRACT

Using renewable energy for power generation is fundamental for obtaining sustainable environment. The most available and widely used source of renewable energy is solar energy. The solar chimney power plant (SCPP) is one of the most important applications of renewable energy technologies for generating electrical energy from solar energy. Basrah city in Iraq is distinguished by a plentiful supply of solar radiation throughout the year, which encourages researchers to use solar energy in a variety of applications, particularly in the generation of electricity. The present article included an experimental study of the SCPP model within the climatic conditions of Basrah, Iraq, to evaluate the behaviour and performance of SCPP system. Many variables that affect the performance of the system are studied, such as solar radiation intensity, solar collector height and chimney height. The best and highest performance of the chimney is recorded experimentally at the height of the chimney and collector are 4.5m and 50mm respectively, where the velocity and available power are 2.5m/s and 57.6mW respectively. While the time at which the best system performance is achieved is between 11:00AM and 1:00PM.

## KEYWORDS

renewable energy, sustainable, solar, chimney.

## INTRODUCTION

An SCPP consists of three components the collector, the chimney and the power conversion power unit (turbine and generator) as shown in figure 1. It is a basic solar thermal power plant with a solar collector that is able to transform solar energy into thermal energy. In the second step, using a combination of a wind turbine and a generator, the produced thermal energy is transformed into kinetic energy in the chimney and eventually into electric energy. The solar radiation is absorbed by the collector and converted to thermal energy. The air inside the collector warms up and finally, with the natural warm air displacement, the thermal power is converted to electrical power by installing a turbine.

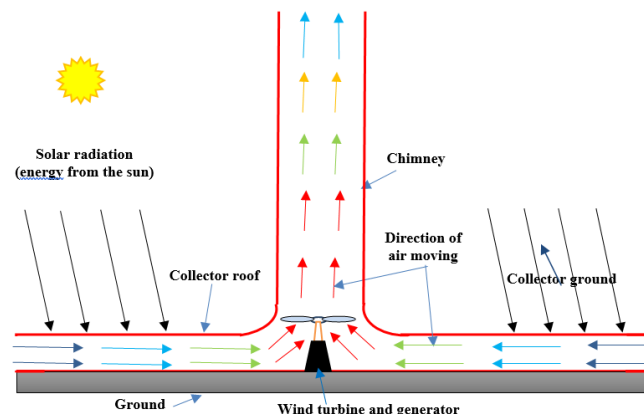


Figure 1. General diagram of SCPP

The first prototype tower was built in Manzanares in 1981, by the team of Professor Schlaich, Haaf et al., [1-2] in Spain. It was worked from 1982 to 1989. The performance calculations for SCPP are important for estimation the best dimensions, location and operating conditions. Perhaps one of the most disadvantages and limitations of a solar chimney is its low efficiency. Therefore, many researchers have tried to address this defect. Therefore, they began to modify and optimize the geometry of the collector and chimney to obtain improved airflow and higher speed. From the studies presented by the researchers during the last 39 years between (1982-2021), it is found that most of these studies were aimed at knowing and improving the performance SCPP by the variation of the factors that affect the performance.

Hammadi [3] presented a mathematical model for studying the influence of several parameters on the SCPP performance such as collector diameter, height and diameter of the chimney, solar radiation and wind velocity according to Basrah climate conditions. Hannun et al. [4] presented a theoretical study to know the impact of the shape of the collector base and also the effect of several storage materials on the SCPP performance. He concluded that a circular collector base and black Pebble storage plate increase the output power of the solar chimney. Hamdan [5] proposed a theoretical model for predicting the performance of an SCPP. This model shows that, as the chimney height and diameter increase the exergy efficiency and power harvested also increase.

Aja et al. [6] showed the influence of wind velocity and wind direction on the performance of solar chimney facing toward south inclination then it was found that the wind velocity had more effect on convective heat loss through the walls and the cover to the ambient. Koonsrisuk and Chitsomboon [7] proposed the use of dimensionless variables to conduct the experimental study of flow in a small scale solar chimney power plant for electricity generation. The similarity of the proposed dimensionless variables is confirmed by computing fluid dynamics. Ali [8] proposed a model of the solar tower and studied the impact of the collector area, chimney height, tower diameter and solar radiation on solar tower power output depending on Manzanares model and climate conditions of Baghdad city in Iraq. He concluded that with the increase of these variables, the output power of the solar chimney increases in varying proportions depending on the variable used.

Khalf [9] developed an SCPP model by using the air intake system at chimney outlet which working by the wind to convert wind energy into useful energy. He concluded that this development in the model design led to an increase in the value of the chimney velocity of the air inside the model, leading to increase the output power of model about (10-15%). This study was conducted according to climatic conditions in Nasiriyah, Iraq. Ghalamchi et al [10] designed a small model of an SCPP at Mehran University in Iran. They studied the effect of the solar collector's height on the performance of the solar chimney. They noticed that the power generated doubles when the collector's height is reduced in half. They also noticed that the highest air velocity within the chimney was 1.30 m/s. Ayadi et al, [11] presented a widespread survey of the properties of an SCPP by employing numerical and experiential method. Their study further confirmed that the collector roof elevation is very principal on the enhancement of the SCPP performance.

In particular, results indicated an improvement in the generated power while reducing the collector roof elevation. Abdelmohimen and Algarni [12] focused on the performance SCPP in six various places in Saudi Arabia was investigated during the year. A numerical model was published with experimental data and used to measure performance. The findings explain that an SCPP with an elevation of 194 m and a collector radius of 122 m can produce an average electric power per month of 56 kW in the city of Riyadh over a year. Ayadi, et al. [13] introduced, a numerical and experimental study of the impact of the obstacles on the distributions of the airflow in an SCPP is presented by using CFD Ansys software. Conclusions cleared that the produced power lightly rises at putting obstacles at the collector output for the considered geometry and under the ambient environmental conditions of the constructed geometry. Jawad et al [14] established a Matlab program with a graphical user interface (GUI) code for studying the performance of an SCPP. The program gives the ability for predicting the performance of SCPP for different geometry dimensions, ambient operating conditions and locations. Also, this program is based on the solution of a mathematical model derived from the heat and mass balance for the system components. The main objective of the present study is to design and construction a

small SCPP prototype in Basra city for performing experimental performance evaluation and knowing the real behavior of this system.

#### Model design of SCPP

The model of SCPP is built and installed on the roof of a house which is located in Iraq, Basrah city, in Hai Al-Jihad, which has the geographical location to be considered for the experimental work is Basrah city, which is on latitude 47.78° N and longitude 30.468° E. The most important basic parameters of this model are listed in table 1 and figure 2.

#### Solar Collector design

The solar collector is one of the main parts of the solar chimney and through it the solar radiation is transmitted. The collector is designed in a horizontal flat circular shape with a radius of 1.5 m for this model. The roof of the collector is covered with transparent glass with a thickness of 4 mm in the form of eight conical pieces. The height of the collector for the first model is 50 mm from the ground and this height is changed to 90 mm to study the effect of changing this height on the performance of the solar chimney. Regarding the collector ground, for this model it is made of aluminium and coated with black paint to increase its heat emission as best as possible, to heat the air under the roof of the collector. Also, a layer of insulation (foam) is placed under the aluminium layer to reduce the heat losses. More details of the designed experimental model are shown in figure 2.

**Table 1.** The Basic parameters for prototype model

| Basic parameters of the prototype                              | Experimental prototype     |
|--|----------------------------|
| Solar collector diameter (m)                                   | 3                          |
| Solar collector height (m)                                     | 0.050 , 0.090              |
| Chimney height (m)   | 3.3 , 4.5                  |
| chimney diameter (m)   | 0.1                        |
| Thickness and net area of solar collector roof (glass)         | 4mm and 6.08m <sup>2</sup> |
| Material and thickness of the chimney                          | PVC (3mm)                  |
| Material and thickness of the chimney insulator                | glass wool ( 50mm)         |
| Material and thickness of the collector ground                 | Aluminium (2mm)            |
| Material and thickness of the insulator under collector ground | Foam (50mm)                |

#### Chimney design

A PVC pipe of 100 mm diameter and 3 mm thickness is used and fixed vertically (by steel wire) in the centre of the solar collector as shown in figure 2. The tube is also insulated with a layer of 5 cm glass wool to reduce the heat lost to the outside environment. In this study, two lengths of the chimney are investigated, namely, 3.3 m and 4.5 m, to assess the effect of increasing the length of the chimney on the performance of the solar chimney.

#### The frame of collector

The frame is designed of iron inverted T-section with a square section (40 mm \* 40 mm) and a thickness of 2 mm and standing on pillars as shown in the figure 4.1. Firstly, the perimeter of the solar collector main circle is formed and secondly dividing the solar collector circle into eight equal parts, extending from the circumference of the collector to the circumference of the base of the chimney in order to represent a base on which the glass is fixed. The base of the chimney is welded to a 20 cm high hollow iron pipe extended from collector roof. The frame also included eight iron pillars welded around the perimeter of the collector in order to support the roof of the collector from its ground by 50 mm and allow the outside air to enter inside the compound

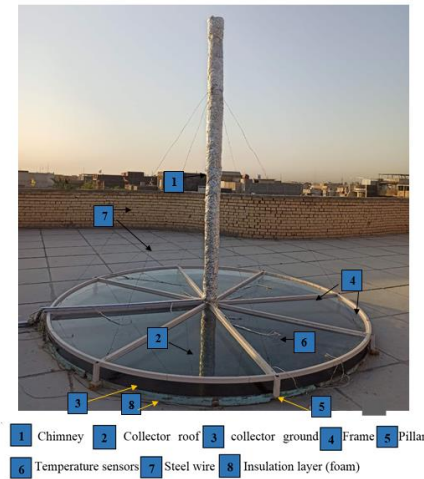


**Figure 2.** Model of SCPP

### Distribution of the temperature measuring points

Electronic temperature sensors are distributed in the designed solar chimney model by installing them in the following location:

*Chimney:* Along the chimney, the temperature is measured at four points. These points have been uniformly fixed in the centre of the chimney (as shown in the figure 2) to measure the temperature of the air flowing through the chimney.

*Solar collector:* Three types of distributions of temperature measuring points, are used separately for the solar collector. For the first type (distribution A), the measuring points are distributed for three concentric circles, in each circle four measuring points are installed for the glass, collector ground, and air in the middle space between the glass and the collector ground. The four measuring points are distributed equally on the circumference of the concentric circles while the distribution of these circles are the same. In addition to measure the temperature of the air entering the collector, four measuring points are installed around the circumference of the collector in the mid-distance of collector height. Also, five measuring points are installed on the bottom of the insulation layer between the ground plate and the earth. Four of those measuring points of the insulation are fixed on the perimeter of the outer circle and the fifth in the centre of the collector. In this type of distribution, 47 measuring points are used (as shown in the figure 3).

The second type of the distribution (distribution B) is illustrated in figure 4. It comprises 53 measuring points. Four measuring points are fixed along the chimney (similar to distribution A). Nine measuring points are fixed on the bottom of the insulation layer uniformly distributed on the circumference along the radial direction. The remainder 40 points are distributed over two circles having 20 points for each one. Each circle includes four points for glass and four points for ground and twelve points are installed along the air passage to measure its temperature. These twelve points are uniformly distributed along the circumference and along the collector height (z-direction). The diameter of each circle is shown in figure 4. The third type of distribution (distribution C) is same as distribution B, except it has 61 points. The additional eight points are added along the collector height. This because in this case, the collector height is greater than those of distribution A and B namely 90mm (as shown in figure 5).

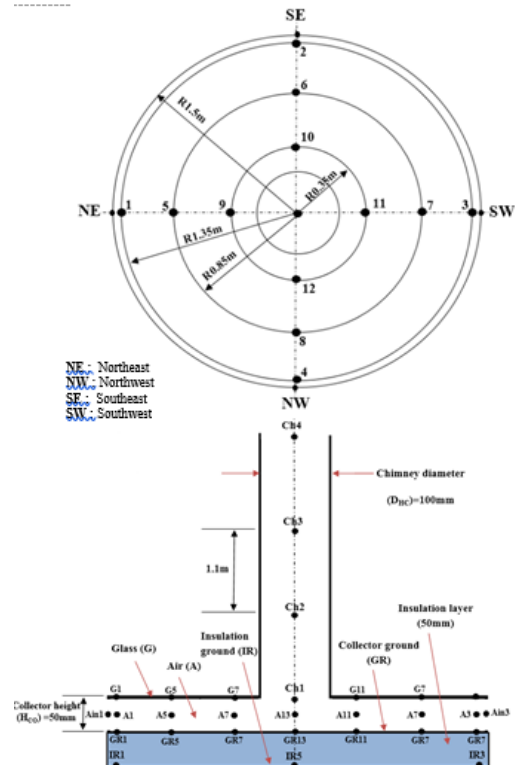


Figure 3. First type of distribution of temperature measuring points (Type A)

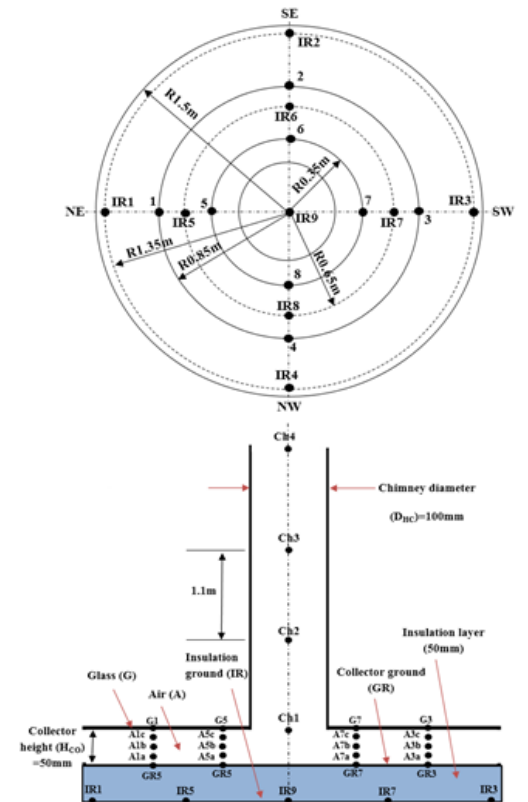


Figure 4. Second type of distribution of temperature measuring points (Type B)

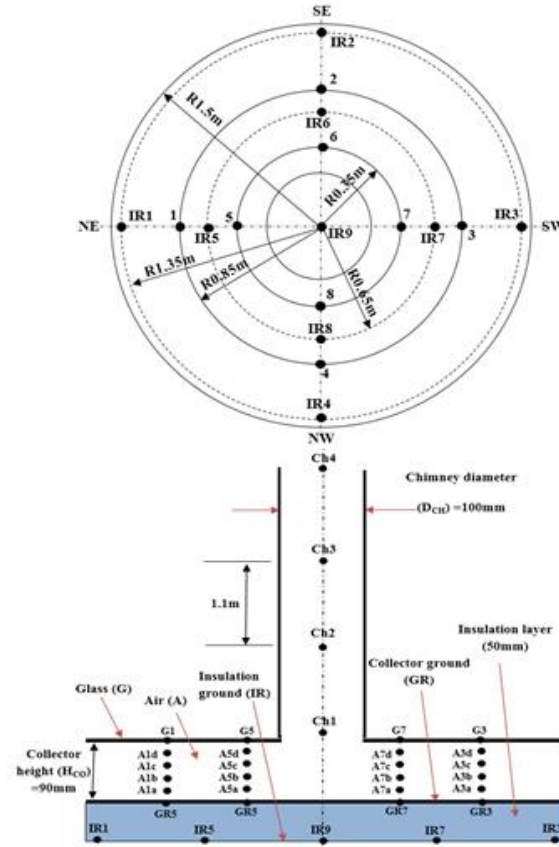


Figure 5. Third type of distribution of temperature measuring points (Type C)

Collecting the data

The measurements are taken during the operation for the experimental model, where the ambient temperature and relative humidity are measured, as well as the wind speed. The total solar radiation falling on the roof of the solar collector is also measured in addition to the measurement of the air velocity in the chimney at a height of 1.5 m from the base of the chimney. The temperatures are also measured for the glass surface, collector and insulator floor, as well as the air in the middle of the collector height. All these measurements are done for 10 hours every day (from 8:00AM until 5:00PM) from 25 June to 15 September during 2020.

In Table 2 some important characteristics of the instruments used in the experimental work are included.

Table 2. Characteristics of the instruments used in the experimental work

| The name and model of the device        | Measured quantity   | Resolution         | Accuracy            | Range                   | Response period |
|---|---------------------|--------------------|---------------------|-------------------------|-----------------|
| Datalogging Solar Power Meter TES-1333R | Solar radiation     | 1 W/m <sup>2</sup> | ±10w/m <sup>2</sup> | 1-2000 W/m <sup>2</sup> | 0.4 s           |
| Digital thermometer TPM-10              | Temperature         | 0.1°C              | ±1°C                | -10-120°C               | 2s              |
| Digital anemometer AR826                | Air velocity        | 0.1m/s             | ±3% ± 0.1dgts       | 0.1-45 m/s              | 0.6s            |
| Mercury thermometer                     | Ambient temperature | 1°C                | -                   | -10-120°C               | -               |

RESULTS AND DISCUSSIONS

The results of this work are conducted experimentally on 20<sup>th</sup> of July 2020. The available power of the solar chimney is based on the relation: [15]:

$$P = 0.5 \cdot \rho \cdot A \cdot V^3 \tag{1}$$

Where:  $\rho$ ,  $A$ ,  $V$ , air density (at location of velocity measurement), cross section area of chimney, and air velocity inside the chimney, respectively.

The collected parameters are gathered in the following subsections.

Temperature distribution in chimney

For collector and chimney heights of 50mm and 3.3m respectively figure 6 shows the distribution of air temperature inside the chimney. The temperature begins to gradually decrease with the height of the chimney, reaching the lowest value at the exit of the chimney. This behaviour of the temperature distribution is almost constant during the day. The air in the chimney inlet has the highest temperature due to its proximity of to the ground of the heated collector. When moving upwards from the entrance to the chimney, the temperature drops due to thermal losses through the wall and the outlet opening of the chimney.

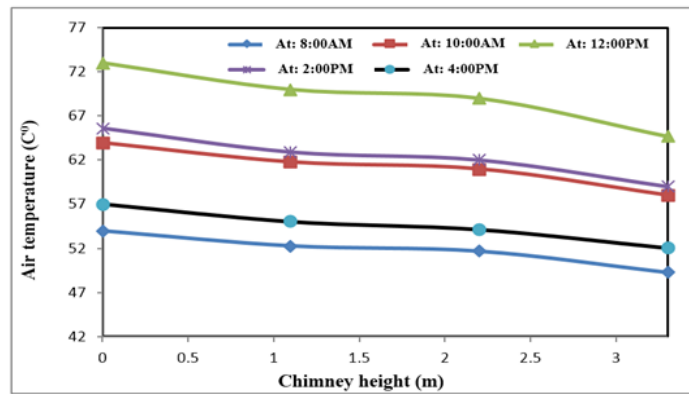


Figure 6. Variation the air temperature distribution inside the chimney with time

Temperature distribution in collector

Figure 7 shows the temperature distribution of the collector ground, where this distribution changes with the location of the measured points radially and azimuthally.

At morning, radially the points are located at the line between the northeast (NE) to southeast (SE) have the greatest temperature than the points located at the line from southwest (SW) to northwest (NW) as shown in figure 3. In the afternoon this behaviour changes are reversed. Points are located in a radius of 0.35 m have a higher temperature than the points in the centre of the collector ground because of shading all the day.

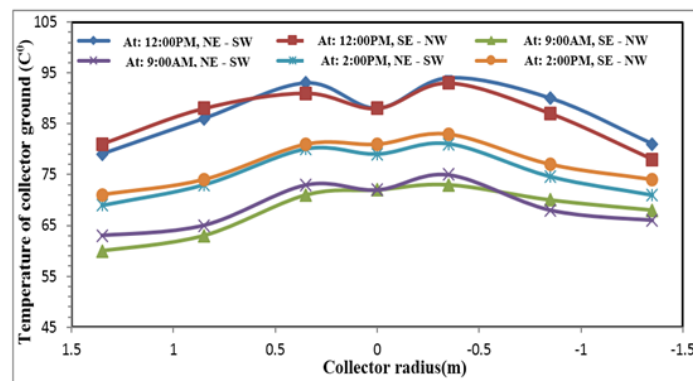


Figure 7. Variation of temperature distribution for collector ground with radial and azimuth

Also, for figure 7, the temperature distribution is according to the first distribution of temperature measurement points (Type A) as shown in Fig. 3 and at the height of collector and chimney are 50mm and 3.3 respectively. Figure 8 shows the distribution of the temperature for the air inside the collector with the three dimensions which are, radius (r), azimuth ( $\theta$ ) and collector height (z). These temperatures are for two values of the radius (0.35m and 0.85m measured from centre), three values for the collector height (12.5mm, 25mm and 37.5 mm) and four values for the azimuth angle ( $\theta$ -direction) which are ( $0^\circ$ ,  $90^\circ$ ,  $180^\circ$  and  $270^\circ$ ). from this figure at  $r = 0.35\text{m}$  and  $r = 0.85\text{m}$ , the temperature decreases with increasing the height from hot ground of the collector. While the temperature increases with the increase of the azimuth angles less than  $180^\circ$  and decreasing with azimuth angles greater than  $180^\circ$  due to the change of the solar location. Also, for constant collector height and azimuth angle the temperature of the air increasing with decreasing radius due to in increase the amount of heat collected with flowing toward the centre. For figure 8, the temperature distribution is according to the second distribution of temperature measurement points (Type B) as shown in Fig. 4 and at the height of collector and chimney are 50mm and 3.3 respectively.

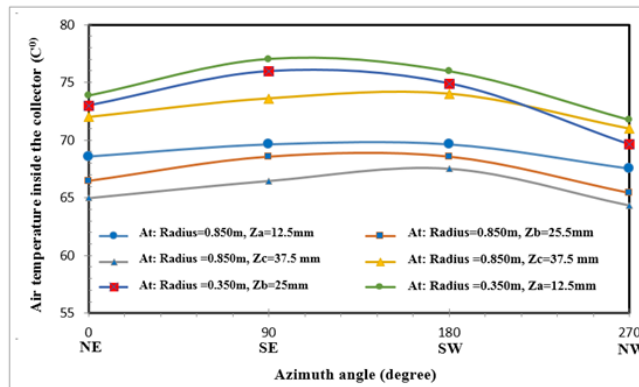


Figure 8. Variation of temperature distribution for air inside the collector at Hco=50mm

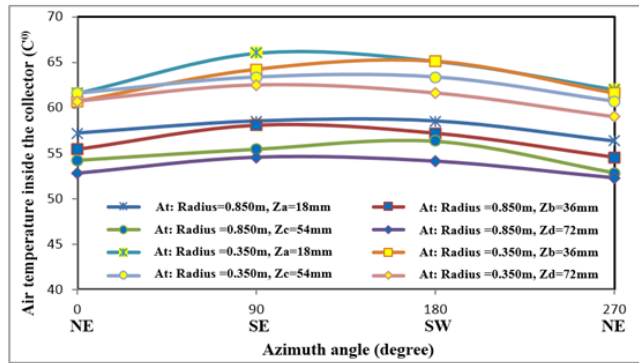


Figure 9. Variation of temperature distribution for air inside the collector at HCO=90mm

Figure 9 shows the similar distribution of air temperature inside the collector but for the collector height is 90mm. the distribution with height are given for four points (18mm, 36mm, 54mm and 72mm). also, the temperature decreasing with increasing the collector height, while the distribution for the radius and the azimuth angle is almost similar to that explained in figure 8. For figure 9, the temperature distribution is according to the third distribution of temperature measurement points (Type C) as shown in Fig. 5 and at the height of collector and chimney are 90mm and 3.3 respectively.

Solar radiation measurement

Due to the importance of the incident solar radiation on the performance of the solar chimney, it has been measured experimentally. The solar radiation falling on the collector ground is also measured by inserting the radiation meter. Table 3 and 4 show the change in the values of solar radiation measured experimentally on the 20th day of July 2020 from 8:00 AM to 5:00 PM. According to Table 3, the measured data includes the solar



radiation falling on the surface of the dusty collector (I), the penetrating radiation falling on the unshaded region of collector ground ( $I_1$ ), and the penetrating radiation falling on the shaded region of collector ground ( $I_2$ ) due to the shade of the collector frame and chimney base.

The shaded ground area of the collector is about 14% of the total area of the collector ground, while the remaining section is the unshaded collector ground area (86% of the total area of the collector ground). Also, this table shows that the maximum values of radiation and the ratios ( $I_1 / I$ ), ( $I_2 / I$ ) are obtained between 11:00AM and 1:00PM o'clock, as well as the highest ratio ( $I_1 / I$ ) and ( $I_2 / I$ ). The average percentage of solar radiation falling on the collector ground  $(0.86*I_1 + 0.14*I_2)/I$  is found to be 46.4%. This average percentage is inversely proportional to the dust covering the collector roof (glass) and the rate of shading the collector ground. To investigate the dust effect the data presented in table 3 are repeated for clean collector roof and depicted in table 4. It is also found that the maximum values of radiation and ( $I_1 / I$ ), ( $I_2 / I$ ) ratios occurs at 11:00AM to 1:00PM. The average percentage of solar radiation falling on the collector ground  $(0.86*I_1 + 0.14*I_2)/I$  is found to be 57.77%.

Depending on the results of Tables 3 and 4, the reasons for the decrease in the amount of solar radiation falling on the collector ground can be explained by several reasons, the most important of which are:

- (i) The reflected radiation from the surfaces.
- (ii) The shading that is spread on the part of the base of the collector.
- (iii) Accumulation of traces and dust on the roof of the solar collector (glass).
- (iv) The angle of sun incidence, which changes during the daytime.

**Table 3.** Data of solar radiation falling on the collector roof dirty with dust

| Time    | I<br>(W/m <sup>2</sup> ) | I <sub>1</sub><br>(W/m <sup>2</sup> ) | I <sub>2</sub><br>(W/m <sup>2</sup> ) | I <sub>1</sub> / I (%) | I <sub>2</sub> / I (%) | (0.86*I <sub>1</sub> +0.14*I <sub>2</sub> )/I (%) |
|---------|--------------------------|---------------------------------------|---------------------------------------|------------------------|------------------------|---|
| 8:00AM  | 695                      | 298.85                                | 62.55                                 | 43                     | 9                      | 38.24   |
| 9:00AM  | 895                      | 465.4                                 | 89.5                                  | 52                     | 10                     | 46.12   |
| 10:00AM | 1040                     | 603.2                                 | 124.8                                 | 58                     | 12                     | 51.56   |
| 11:00AM | 1125                     | 697.5                                 | 157.5                                 | 62                     | 14                     | 55.28   |
| 12:00PM | 1166                     | 734.58                                | 174.9                                 | 63                     | 15                     | 56.24   |
| 1:00PM  | 1130                     | 700.6                                 | 158.2                                 | 62                     | 14                     | 55.28   |
| 2:00PM  | 1000                     | 570                                   | 130                                   | 57                     | 13                     | 50.84   |
| 3:00PM  | 835                      | 417.5                                 | 91.85                                 | 50                     | 11                     | 44.54   |
| 4:00PM  | 615                      | 258.3                                 | 55.35                                 | 42                     | 9                      | 37.38   |
| 5:00PM  | 370                      | 118.4                                 | 25.9                                  | 32                     | 7                      | 28.5  |
| Average | 887.1                    | 486.43                                | 107                                   | 52.1                   | 11.4                   | 46.4  |

**Table 4.** Data of solar radiation falling on the clean collector roof

| Time    | I<br>(W/m <sup>2</sup> ) | I <sub>1</sub><br>(W/m <sup>2</sup> ) | I <sub>2</sub><br>(W/m <sup>2</sup> ) | I <sub>1</sub> / I (%) | I <sub>2</sub> / I (%) | (0.86*I <sub>1</sub> +0.14*I <sub>2</sub> )/I (%) |
|---------|--------------------------|---------------------------------------|---------------------------------------|------------------------|------------------------|---|
| 8:00AM  | 695                      | 326.65                                | 76.45                                 | 47                     | 11                     | 41.69   |
| 9:00AM  | 895                      | 537                                   | 134.25                                | 60                     | 15                     | 53.7  |
| 10:00AM | 1040                     | 780                                   | 187.2                                 | 75                     | 18                     | 67.02   |
| 11:00AM | 1125                     | 922.5                                 | 225                                   | 82                     | 20                     | 73.32   |
| 12:00PM | 1166                     | 991.1                                 | 256.52                                | 85                     | 22                     | 76.18   |
| 1:00PM  | 1130                     | 937.9                                 | 237.3                                 | 83                     | 21                     | 74.32   |
| 2:00PM  | 1000                     | 730                                   | 180                                   | 73                     | 18                     | 65.3  |
| 3:00PM  | 835                      | 492.65                                | 116.9                                 | 59                     | 14                     | 52.7  |
| 4:00PM  | 615                      | 282.9                                 | 61.5                                  | 46                     | 10                     | 40.96   |
| 5:00PM  | 370                      | 125.8                                 | 29.6                                  | 34                     | 8                      | 30.36   |
| Average | 887.1                    | 612.65                                | 150.74                                | 64.4                   | 15.7                   | 57.55   |

Temperature difference measurement

Figure 10 portrays the difference between the temp. at the entrance of the chimney and the ambient temperature along the day for different collector and chimney heights. Generally, the maximum temperature difference is recorded of 11:00AM to 1:00PM. It is observed from this figure, that the longer chimney and the shorter height of the collector give the higher temp. difference. Also, decreasing the collector height increasing the temperature difference due to decrease the mass flow of entering air. The maximum percentage increase in the temperature difference between 8:00AM and 1:00PM is about 2% for  $H_{CO} = 50\text{mm}$  and  $H_{CH} = 4.5\text{m}$ .

Velocity variation inside the chimney

In figure 11, the trend of daily velocity variations for the same parameters of figure 10 is almost similar to that of temp. distribution shown in figure 10. This is due to the correlated air velocity with the buoyancy force. The percentage increase in the air velocity between 8:00AM and 1:00PM is about 1.08% for  $H_{CO} = 50\text{mm}$  and  $H_{CH} = 4.5\text{m}$ , while for  $H_{CO} = 90\text{mm}$  and  $H_{CH} = 3.3\text{m}$  the percentage is about 0.88%.

Power variations

As given in equation 1, the available power is proportional with the cubic air velocity. The daily variations in the available power with time is shown in figure 12. The figure demonstrates that, maximum available power between 11:00AM and 1:00PM. The percentage increase of the available power between 8:00AM and 1:00PM is about 3.97% for  $H_{CO} = 50\text{mm}$  and  $H_{CH} = 4.5\text{m}$ , while for  $H_{CO} = 90\text{mm}$  and  $H_{CH} = 3.3\text{m}$  the percentage is about 3.28%. From the above figures (10,11 and 12), it is clearly evident that the time period that gives the greatest power and velocity of the SCPP is between 11:00AM to 1:00PM during 20<sup>th</sup> of July. At height of collector and chimney 50mm and 4.5 respectively, the greatest values are recorded for the speed and temperature difference are 2.5m/s and 24C<sup>0</sup>, respectively, while the calculated available power is 57.6 mW as shown in table 5.

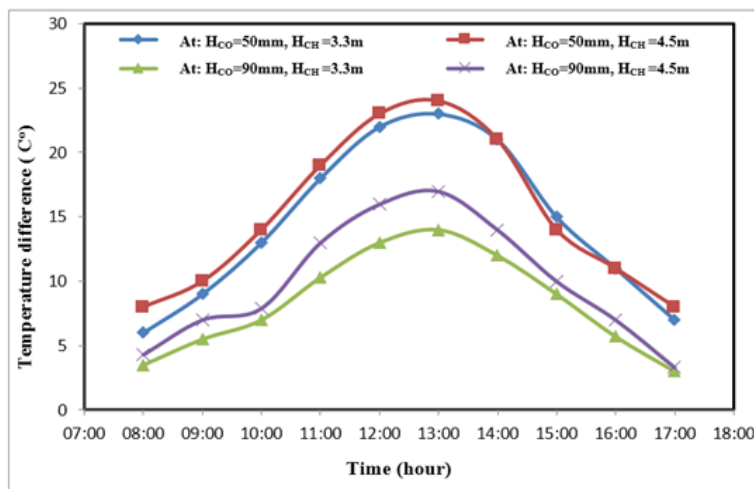


Figure 10. Variation of temperature difference with time

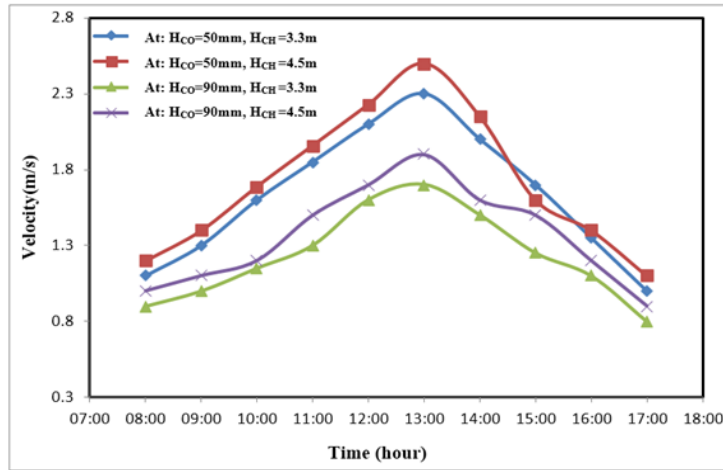


Figure 11. Variation of air velocity in chimney with time

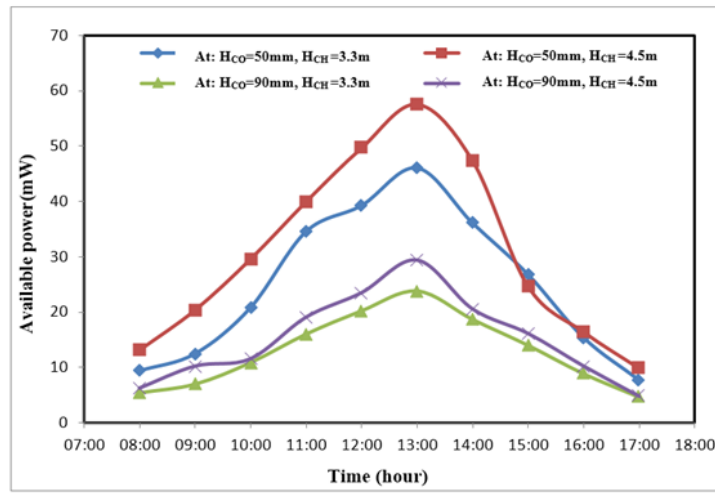


Figure 12. Variation of available power with time

Table 5. Parameters comparison among different height of collector and chimney

| Collector height (mm) | Chimney height (m) | Maximum air temperature inside collector(C <sup>0</sup> ) | Maximum velocity (m/s) | Maximum available power (mW) |
|-----------------------|--------------------|---|------------------------|------------------------------|
| 50                    | 3.3                | 77  | 2.3                    | 46                           |
| 50                    | 4.5                | 79  | 2.5                    | 57.6                         |
| 90                    | 3.3                | 66  | 1.8                    | 23.8                         |
| 90                    | 4.5                | 68  | 1.95                   | 29.4                         |

CONCLUSIONS

The main conclusions that can be obtained from this work are summarized as follows:

- 1- The best and highest performance of the chimney is recorded experimentally at the height of the chimney is 4.5m and the height of the collector is 50mm, where the velocity and power are 2.5m/s and 57.6mW respectively. While the time at which the best system performance is achieved is between 11:00AM and 1:00PM.
- 2- By using a large number of temperature sensors, the behaviour of the temperature distribution in the SCPP system is more accurate and visualized in the three dimensions.

3- Experimentally, the percentage range of total radiation falling on the collector ground is 57.77% of the value of radiation falling on the clean collector roof (glass) while, it is 46.4% of the value of radiation falling on the dust collector roof. Also, the lowest losses of solar radiation falling on the collector obtained at the midday, as well as when the collector's glass is clean.

4- Basrah city conditions are good for operating of SCPP.

#### REFERENCES

- [1] W. Haaf, K. Friedrich, G. Mayr and J. Schlaich, "Solar Chimneys. Part 1: Principle and Construction of the Pilot Plant in Manzanares", *International Journal of Solar Energy*, Vol. 2, Issue 1, pp. 3-20, 1983.
- [2] W. Haaf, K. Friedrich, G. Mayr and J. Schlaich, "Solar Chimneys, Part II: Preliminary Test Results From the Manzanares Pilot Plant", *International Journal of Solar Energy* 2, pp. 141–161, 1984.
- [3] S. H. Hammadi, "Solar Chimney Power Plant in Basrah", *Basrah Journal for Engineering Sciences*, Vol. 9, Issue 1, pp. 1-8, 2009.
- [4] R. M. Hannun, A. U. Adnan and G. A. Abd, "Prediction of Power Chimney Parameters Influenced the Operation at Nassiriya City", *Thi-Qar University Journal for Engineering Sciences*, Vol. 2, Issue 2, 2011.
- [5] M. O. Hamdan, "Analysis of a solar chimney power plant in the Arabian Gulf region", *Renewable Energy*, Vol. 36, No. 10, pp. 2593-2598, 2011.
- [6] O. C. Aja, H. H. Al-Kayiem and Z. A. Abdul Karim, "Experimental investigation of the effect of wind speed and wind direction on a solar chimney power plant", *8th International Conference on Urban Regeneration and Sustainability*, Putrajaya, Malaysia, 2013.
- [7] A. Koonsrisuk and T. Chitsomboon, "Accuracy of theoretical models in the prediction of solar chimney performance", *Solar Energy*, Vol. 83, Issue 10, pp. 1764-1771, 2009.
- [8] M. H. Ali, "Analysis Study of Solar Tower Power Plant and Its Configuration Effects on Its Performance in Iraq (Baghdad City)", *Modern Applied Science*; Vol. 7, No. 4, 2013.
- [9] M.H. Khalf , " Modeling of hybrid solar-wind power chimney" , M.Sc. thesis, University of Basrah, Mechanical Engineering Department, Basrah, 2014.
- [10] Ghalamchia, M., Kasaeian A. Ghalamchia M., "Experimental study of geometrical and climate effects on the performance of a small solar chimney", *Renewable and Sustainable Energy Reviews*, 43, pp. 425–431, 2015.
- [11] A. Ayadi, A. Bouabidi, Z. Driss , , M.S. Abid, "Experimental and numerical analysis of the collector roof height effect on the solar chimney performance", *Renewable Energy*, , 115: pp. 649-662, 2018.
- [12] M. A. H., Abdelmohimen, S. A. Algarni, "Numerical investigation of solar chimney power plants performance for Saudi Arabia weather conditions", *Sustainable Cities and Society*, Vol. 38, pp. 1–8, 2018.
- [13] A. Ayadi, Z. Driss, M. S. Abid , "The impact of placing obstacles on the distribution of the airflow inside a solar chimney" , *Environ Prog Sustainable Energy*, 39:e13379, 2020.
- [14] I. N. Jawad, Q. A. Rishack, H. S. Sultan, "Matlab graphical user interface (GUI) code for solar tower power plant performance calculations" , *Basrah Journal for Engineering Sciences*, Vol. 21, No. 1, (2021), 8-14, No. 1, pp. 8-14, 2021.
- [15] FP. Incropera, DP. DeWitt, TL.Bergman, AS. Lavine. *Introduce to heat transfer*.4th ed.NewYork:Wiley;1934.